

## CALCULATION OF THE INTEGRAL OPTICAL CHARACTERISTICS OF A SODIUM PLASMA

S. S. Katsnel'son

UDC 536.45

*The emissivities of a plane layer and a hemispherical volume and also the Planck and Rosseland mean values of a sodium plasma are calculated in the range of temperatures 1000–20,000 K and pressures 0.1–20 bar. In determination of the spectral coefficient of absorption the entire spectral interval in which the main part of radiant energy is transferred is taken into account, and also the most important radiation processes that are associated with free–free, bound–free, and bound–bound transitions are considered. For the first time, the effect of internal microfields in the plasma is taken into account, thus allowing a correct calculation of the populations of excited states, shift of ionization equilibrium, and a smooth transition of the line spectrum into a continuous one in the near-threshold regions.*

Calculation of radiation energy transfer is reduced to the determination of the divergence of the total radiation flux, which is associated with the necessity of solving the equation of transfer for the spectral intensity:

$$\vec{\Omega} \text{ grad } I_{\nu} = K'_{\nu} (I_{\nu p} - I_{\nu}),$$

integrated with respect to the angles and frequency. This problem involves great mathematical difficulties, and therefore the methods of its solution that use these or other assumptions and first of all limiting approximations have gained wide acceptance in practice. The latter include the replacement of real radiating volumes by homogeneous ones, the assumption about a very low or high optical density of gas volumes, or their combination.

**Homogeneous Models. Emissivities.** Homogeneous models are used in those cases where it is required to evaluate the radiation flux escaping from a volume and the volume itself does not differ greatly from a homogeneous one. The spectral flux of the radiant energy incident on a unit area isolated at the boundary of the radiating volume is determined most simply for a plane layer and a hemispherical volume [1, 2].

The contribution of separate portions of the spectrum to the total balance of radiant losses can be characterized by means of the so-called emissivity, defined as

$$\varepsilon = \int_{\Delta\nu} S_{\nu} d\nu / \sigma T^4. \quad (1)$$

The emissivities of the plane layer and of the hemispherical volume are

$$\varepsilon^{\text{pl}} = \int_{\Delta\nu} S_{\nu p} (1 - 2E_3(\tau_{\nu})) d\nu / \sigma T^4, \quad (2)$$

$$\varepsilon^{\text{sph}} = \int_{\Delta\nu} S_{\nu p} (1 - \exp(-\tau_{\nu})) d\nu / \sigma T^4, \quad \tau_{\nu} = K_{\nu} l. \quad (3)$$

---

Institute of Theoretical and Applied Mechanics, Siberian Branch of the Russian Academy of Sciences, Novosibirsk, Russia. Translated from *Inzhenerno-Fizicheskii Zhurnal*, Vol. 73, No. 5, pp. 945-952, September–October, 2000. Original article submitted January 5, 1999; revision submitted February 21, 2000.

**Planck and Rosseland Approximations.** In some problems, the entire spectrum or a great portion of it can be transparent to radiation, i.e., the length of the mean free path of photons is much larger than the characteristic dimensions of the region  $L$ , which is the condition of volumetric luminescence of light:

$$l_v \sim 1/K'_v \gg L \quad \text{and} \quad \tau_v = \int K'_v dx \sim K'_v L \ll 1.$$

In this case, the divergence of the radiation flux can be determined as

$$\operatorname{div} \vec{S} = 4\sigma T^4 k_{\text{Pk}}, \quad (4)$$

where

$$k_{\text{Pk}} = \int_0^\infty K'_v U_{\text{vp}} dv / \int_0^\infty U_{\text{vp}} dv \quad (5)$$

is the mean coefficient of absorption (the Planck mean value).

The Rosseland approximation (the approximation of radiative heat conduction) is valid for regions of large geometric dimensions or with a high density of particles when a considerable portion of radiation is closed within the region, i.e., the path length of the photons is much smaller than the characteristic geometric dimension. In this case, radiation is nearly isotropic and the radiant energy flux is

$$\vec{S} = -\kappa \operatorname{grad} T, \quad \kappa = \frac{16\sigma l_{\text{Ros}} T^3}{3}, \quad (6)$$

where

$$l_{\text{Ros}} = \int_0^\infty \frac{1}{K'_v} \frac{dU_{\text{vp}}}{dT} dv / \int_0^\infty \frac{dU_{\text{vp}}}{dT} dv \quad (7)$$

is the mean free path length of radiation (the Rosseland mean value).

**Calculation of the Spectral Coefficient of Absorption.** The base of calculation of radiative field and radiant heat exchange is the spectral coefficient of absorption. The latter is determined by the free-free transitions of an electron in the fields of ions and neutrals (braking processes), bound-free transitions (photoionization, photoseparation, etc.), and bound-bound transitions. The first two types of transitions form a continuous spectrum, whereas the bound-bound transitions form a discrete spectrum (spectral lines). For practical calculations of the absorption coefficient  $K_v$  in a continuous spectrum, the Biberman-Norman integral formulas have gained widespread use [3, 4]. In [5-7] the Biberman-Norman formulas were refined due to the allowance for the perturbing effect of charged particles in the plasma on its composition and optical properties. The expression for the absorption coefficient in a continuous spectrum in inverse centimeters has the form [7]

$$K_{\text{vcon}} = CZ^2 \frac{n_e n_i}{\sqrt{T}} \frac{\xi(v)}{v^3} (1 + W \exp(-\Delta I/kT) F), \quad (8)$$

$$F = \begin{cases} \exp(h(v + \Delta v_{\text{opt}})/kT) - 1, & \text{if } v < v_{\text{thr}} - \Delta v_{\text{opt}}, \\ \exp(hv_{\text{thr}}/kT) - 1, & \text{if } v \geq v_{\text{thr}} - \Delta v_{\text{opt}}. \end{cases}$$

Here  $C = \frac{4\sqrt{2\pi}}{3\sqrt{3}} \frac{e^6}{\cosh m_e^{3/2} k^{1/2}} = 0.368 \cdot 10^9$  and  $\nu_{\text{thr}}$  is the frequency of the threshold level of the atom starting with which all the higher-lying levels are taken into account integrally.

The probability of the implementation of this state (or a correction to its statistical weight) is the integral of the function of the microfield in the plasma  $W = \int_0^{\beta_n} p(\beta_n, a) d\beta$ , where  $p(\beta_n, a)$  is Hooper's function of the microfield [8]. According to [9], the dimensionless intensity  $\beta_n$  and parameter  $a$  are  $\beta_n = E/E_0$  and  $a = r_0/D$ . The intensity of the microfield causing the decrease of the barrier to the height  $\epsilon_n$  is  $E = (\epsilon_n^2/e^3)Z/(\sqrt{Z^*} + \sqrt{Z})^4$ . The integrals of Hooper's function of the microfield calculated for a neutral atom and a singly charged ion are given in [10]. The value of  $W(\beta_n, a)$  is calculated from the frequency  $\nu(h\nu = \epsilon_n)$  for  $\nu < \nu_{\text{thr}}$  and from the frequency  $\nu_{\text{thr}}$  for  $\nu \geq \nu_{\text{thr}}$ .

The contribution to the absorption coefficient due to photoionization from the levels that lie below the threshold one is taken into account individually:

$$K_{\nu n} = \sigma_n(\nu) n_n \left( \frac{\nu_n}{\nu} \right)^3, \quad \nu \geq \nu_n - \Delta\nu_{\text{opt}0}. \quad (9)$$

The overall absorption coefficient in a continuous spectrum with allowance for the forced emission is

$$K'_{\text{vcon}} = \left( K_{\text{vcon}} + \sum_n K_{\nu n} \right) [1 - \exp(-h\nu/kT)]. \quad (10)$$

The absorption coefficient for a solitary spectral line is determined by the expression [11]

$$K'_{\text{vline}} = \frac{S_{\text{line}} \sqrt{\ln 2}}{\sqrt{\pi} \Delta\nu_{\text{Dop}}} \frac{a}{\pi} \int_{-\infty}^{\infty} \frac{\exp(-t^2) dt}{a^2 + (x-t)^2}. \quad (11)$$

Here  $S_{\text{line}} = \frac{\pi e^2}{m_e c} n_n f_{ij} (1 - \exp(-h\nu/kT))$ ;  $\Delta\nu_{\text{Dop}} = \frac{\sqrt{2kT \ln 2}}{mc^2} \nu_0$ ;  $a = \frac{\Delta\nu_{\text{im}} \sqrt{\ln 2}}{\Delta\nu_{\text{Dop}}}$ ;  $x = (\nu - \nu_0) \sqrt{\ln 2} / \Delta\nu_{\text{Dop}}$ ;  $\nu_0 = \nu_0 + d_{\text{St}}$ ;  $\Delta\nu_{\text{imp}} = \Delta\nu_{\text{St}} + \Delta\nu_{\text{nat}} + \Delta\nu_{\text{eq}}$ ;  $\Delta\nu_{\text{nat}} = \frac{2\pi e^2 (\nu_0')^2}{3m_e c^3}$ ;  $\Delta\nu_{\text{eq}} = \frac{5.48}{16\pi} \frac{\sqrt{g_0}}{g_n} \frac{e^2 f_{0n}}{m_e \nu_0} n_0$ .

In [12], an approximate expression of the absorption coefficient determined by Eq. (11) is given:

$$K'_{\text{vline}} = \frac{S_{\text{line}} \sqrt{\ln 2}}{\sqrt{\pi} \gamma} (1 - \xi) \exp(-\eta^2 \ln 2) + \frac{S_{\text{line}}}{\pi \gamma} \frac{\xi}{1 + \eta^2} - \frac{S_{\text{line}}}{\pi \gamma} \xi (1 - \xi) \left( \frac{1.5}{\ln 2} + 1 + \xi \right) \left[ 0.066 \exp(-0.4\eta^2) - \frac{1}{40 - 5.5\eta^2 + \eta^4} \right], \quad (12)$$

where

$$\gamma = \frac{1}{2} (\Delta\nu_{\text{imp}} + \sqrt{\Delta\nu_{\text{imp}}^2 + 4\Delta\nu_{\text{Dop}}^2}) + 0.05 \Delta\nu_{\text{imp}} \left( 1 - \frac{2\Delta\nu_{\text{imp}}}{\Delta\nu_{\text{imp}} + \sqrt{\Delta\nu_{\text{imp}}^2 + 4\Delta\nu_{\text{Dop}}^2}} \right);$$

$$\eta = \frac{v - v_0^1}{\gamma}; \quad \xi = \frac{\Delta v_{\text{imp}}}{\gamma}.$$

As is shown in [7], as a result of the allowance for the microfields in the plasma the intensity of the spectral lines decreases as they converge to the boundaries of the corresponding series due to the decrease in the probability of the realization of the upper discrete state.

**Calculation of the Composition.** For a singly ionized gas the equation of state can be written in the form [1]

$$p = (1 + \alpha) nkT, \quad n_i = n_e = \alpha n, \quad n_0 = (1 - \alpha) n.$$

The degree of ionization  $\alpha$  is determined by the Saha equation:

$$\frac{\alpha^2}{1 - \alpha^2} = A \frac{\sum_1 T^{5/2}}{\sum_0 p} \exp\left(-\frac{I - \Delta I}{kT}\right), \quad A = 2 \left(\frac{2\pi m_e k^{5/3}}{h^2}\right)^{3/2}.$$

According to [6], the statistical sum of the atom (ion) over electron states with allowance for the microfield has the following form:

$$\Sigma = \sum_{n=0}^{\infty} W(\beta_n, a) g_n \exp(-\varepsilon_n/kT).$$

The summation must be done over all the levels, but practically it is possible to restrict oneself to a small number of terms, since the contribution of the terms with a large  $n$  tends to zero because of the smallness of  $W(\beta_n, a)$ .

**Calculation Results.** The spectral absorption coefficient of the sodium plasma was calculated on the final frequency interval of  $(0.01-6) \cdot 10^{15} \text{ sec}^{-1}$  since, according to the estimates, no more than 0.1% of all the energy is transferred beyond this interval. The regions of change in the temperatures and pressures were prescribed by the intervals of  $(1-20) \cdot 10^3 \text{ K}$  and  $(0.1-30) \text{ bar}$ , respectively.

The absorption coefficient of the continuous spectrum was calculated from formulas (8)-(10). The threshold frequency was assigned equal to  $v_{\text{thr}} = 0.36806 \cdot 10^{15} \text{ sec}^{-1}$ . The optical shift was calculated from the Inglis-Teller formula [13]:  $\Delta v_{\text{opt}} = 0.1566 n_e^{1/2} \cdot 10^{15} \text{ sec}^{-1}$ . The values of the function  $\xi(v)$  are taken from [3, 14] for the infrared and visible parts of the spectrum and from [4] for the violet part, where, according to [3],  $\xi(v)$  is close to the corresponding function for neon.

The photoionization from the 4s, 3p, and 3s levels was taken into account individually. The cross sections for photoionization  $\sigma_{4s}(v)$  and  $\sigma_{3p}(v)$  are taken from [14] and  $\sigma_{3s}(v)$  from [3]. The threshold frequencies are respectively equal to  $v_1 = 0.47098 \cdot 10^{15} \text{ sec}^{-1}$ ,  $v_2 = 0.7343 \cdot 10^{15} \text{ sec}^{-1}$ , and  $v_3 = 1.24266 \cdot 10^{15} \text{ sec}^{-1}$ .

In the calculation of the spectral coefficient of absorption of the discrete spectrum, the transitions between the terms  $^2S$ ,  $^2P^0$ , and  $^2D$  were taken into account. The scheme of the terms of the Na I atom is presented in Fig. 1. The arrows show the most important transitions (doublets) that were taken into account in the calculations. The calculations were carried out by formulas (11) and (12). The data to calculate the Stark halfwidths  $\Delta v_{S_i}$  and Stark shift  $d_{S_i}$  are taken from [15, 16], and the oscillator strengths and the statistical weights of the states are taken from [17, 18].

The procedure of calculating the spectral absorption coefficient for each set of parameters  $p$  and  $T$  was preceded by splitting of the initial spectral interval. To calculate  $K'_{\text{vcon}}$ , each of the four frequency intervals formed by the boundaries of the initial interval and displaced by the thresholds of the 4s, 3p, and 3s levels was split into 50 equal intervals, and the points obtained in this way were fixed. To calculate  $K'_{\text{vline}}$  the displaced centers of the lines and the respective overall halfwidths  $\Delta v_{\text{over}} = \Delta v_{\text{imp}} + \Delta v_{\text{Dop}}$  of the lines were determined,

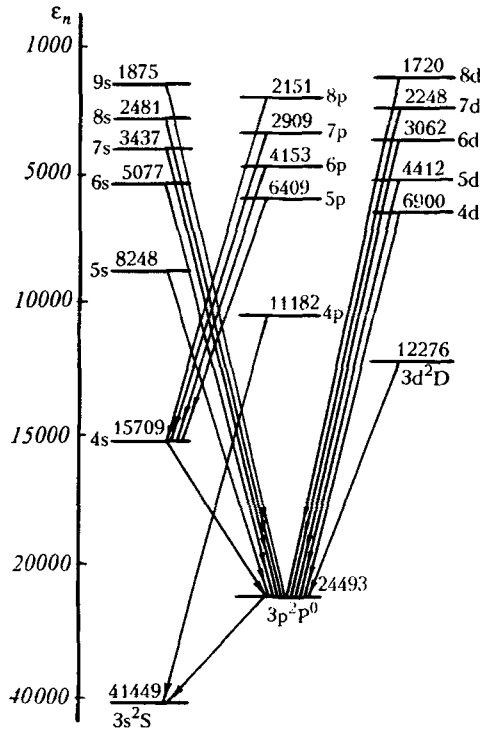


Fig. 1. Scheme of terms and incorporated transitions for a sodium atom.  $\epsilon_n, \text{cm}^{-1}$ .

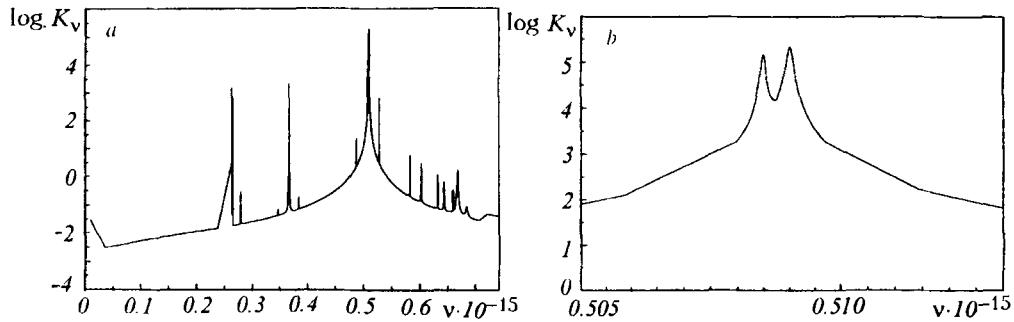


Fig. 2. Coefficient of absorption of a group of the strongest lines (a) ( $p = 1.0 \text{ bar}, T = 3000 \text{ K}$ ) and contours of the lines of the yellow-orange doublet (b) (from series a).  $K_v, \text{cm}^{-1}; \nu, \text{sec}^{-1}$ .

and then the splitting of the frequency interval was carried out on both sides of the centers on the halfwidth  $\Delta\nu_{\text{over}}$  into 10 intervals with the step  $\Delta\nu_{\text{over}}/10$  and thereafter into 10 intervals with the step  $\Delta\nu_{\text{over}}$ . The final splitting was determined by respective combination of the points of the continuous and discrete spectra, precisely in which the overall spectral coefficient of absorption was calculated. Figure 2a presents a fragment of calculation of the spectral absorption coefficient for  $p = 1.0 \text{ bar}$  and  $T = 3000 \text{ K}$  over the spectral interval that contains a group of the strongest lines, and Fig. 2b of the same series presents the contours of broadened and mutually overlapping lines of the yellow-orange doublet.

On the basis of the spectral coefficient of absorption, we calculated the integral optical characteristics: emissivity of the plane layer and of the hemispherical volume for thicknesses of 0.1, 1.0, 1.5, 2.0, 5.0, 10, 20, 30, and 100 cm and also the Planck and Rosseland mean path lengths. Table 1 presents the Planck mean value  $k_{Pk}$  in inverse centimeters and the Rosseland mean value  $l_{Ros}$  in centimeters.

TABLE 1. Planck  $k_{pk}$  and Rosseland  $l_{Ros}$  Mean Values

T, K	p, bar					
	0.10	0.29	0.83	2.40	6.93	20.00
	$k_{pk}$					
1000	.762E-03	.600E-02	.491E-01	.407E+00	.338E+01	.281E+02
1310	.579E-02	.174E-01	.705E-01	.386E+00	.264E+01	.204E+02
1720	.119E+00	.296E+00	.820E+00	.247E+01	.831E+01	.338E+02
2250	.936E+00	.227E+01	.605E+01	.172E+02	.503E+02	.153E+03
2950	.329E+01	.794E+01	.208E+02	.581E+02	.167E+03	.486E+03
3870	.591E+01	.147E+02	.381E+02	.106E+03	.303E+03	.874E+03
5080	.429E+01	.127E+02	.381E+02	.112E+03	.100E+01	.964E+03
6660	.609E+00	.337E+01	.152E+02	.584E+02	.100E+01	.621E+03
8730	.323E-01	.234E+00	.159E+01	.941E+01	.100E+01	.197E+03
11400	.193E-02	.144E-01	.108E+00	.793E+00	.994E+00	.309E+02
15000	.146E-03	.107E-02	.856E-02	.690E-01	.817E+00	.362E+01
19700	.142E-04	.108E-03	.866E-03	.762E-02	.432E+00	.426E+00
	$l_{Ros}$					
1000	.134E+04	.161E+03	.193E+02	.232E+01	.278E+00	.334E-01
1310	.201E+04	.242E+03	.291E+02	.349E+01	.419E+00	.503E-01
1720	.288E+04	.346E+03	.415E+02	.499E+01	.599E+00	.720E-01
2250	.378E+04	.456E+03	.550E+02	.663E+01	.798E+00	.961E-01
2950	.429E+04	.538E+03	.660E+02	.801E+01	.969E+00	.117E+00
3870	.136E+04	.273E+03	.476E+02	.723E+01	.101E+01	.136E+00
5080	.228E+03	.508E+02	.102E+02	.227E+01	.486E+00	.110E+00
6660	.367E+03	.684E+02	.124E+02	.243E+01	.539E+00	.136E+00
8730	.444E+04	.559E+03	.736E+02	.112E+02	.187E+01	.387E+00
11400	.558E+05	.676E+04	.771E+03	.980E+02	.126E+02	.187E+01
15000	.442E+06	.538E+05	.602E+04	.733E+03	.840E+02	.103E+02
19700	.833E+07	.906E+06	.978E+05	.892E+04	.794E+03	.598E+02

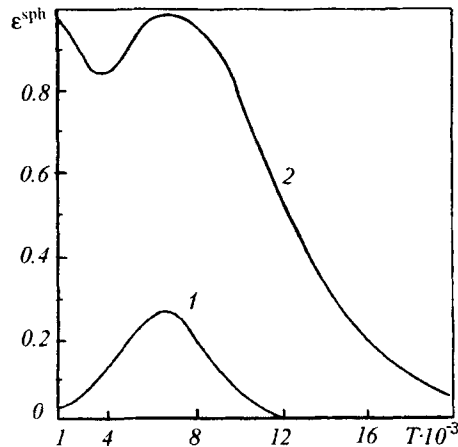


Fig. 3. Emissivity of a hemispherical volume ( $l = 1$  cm) vs. temperature for the pressures: 1)  $p = 0.1$  bar; 2) 11.72. T, K.

To be able to use interpolation formulas in the logarithmic variables that are most frequently used in practical calculations, we obtained the integral optical characteristics in logarithmically uniform scales over  $T$  and  $p$  for temperatures from 1000 to 20,000 K and pressures from 0.1 to 20 bar.

We note certain specific features of the integral characteristic using the radiation from a hemispherical volume as an example. Figure 3 presents temperature dependences of the emissivity of the hemispherical vol-

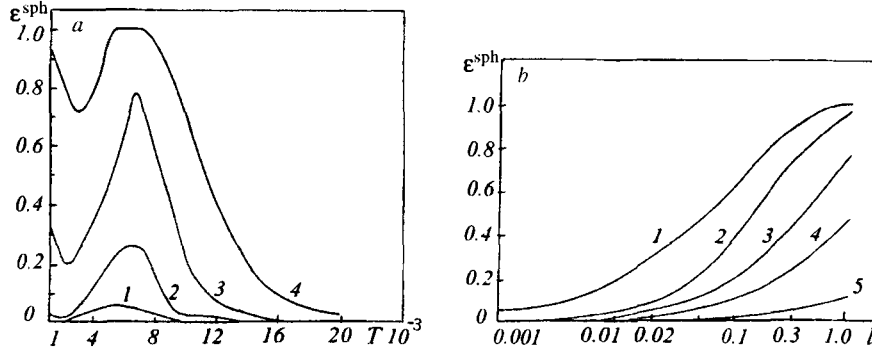


Fig. 4. Emissivity of a hemispherical volume ( $p = 0.8$  bar) vs. temperature for the radii (a): 1)  $l = 0.1$  cm; 2) 1.0; 3) 10; 4) 100 and vs. radius for the temperatures (b): 1) 5000 K; 2) 1000; 3) 2250; 4) 11,400; 5) 15,000.  $T$ , K.

ume. It is seen that  $\epsilon^{\text{sph}}$  has a pronounced nonmonotonic character. This is typical of the radiation of the plasma of all the alkali metals that have a low ionization potential [19]. At low temperatures the main contribution to the radiation is made by the discrete spectrum. As the temperature increases, the population of the upper excited states decreases rapidly; moreover, at  $p = \text{const}$  the gas density decreases and the role of the line spectrum in the absorption coefficient decreases, which leads to a decrease in  $\epsilon^{\text{sph}}$ . This is especially evident for high pressures ( $p \geq 10$  bar). The decrease in  $\epsilon^{\text{sph}}$  continues until the role of photoionization processes becomes prevailing. From this instant and up to  $T \sim 6500\text{--}7000$  K, up to complete ionization, the temperature increase leads to an increase in the emissivity. With further increase in the temperature an illumination of the plasma due to the decrease in the density is observed. As the radius of the hemispherical volume  $l$  increases, the nonmonotonicity of the profile of  $\epsilon^{\text{sph}}$  increases (Fig. 4a). Figure 4b presents the dependence of the emissivity on  $l$  for different temperatures. Here, in addition to the obvious fact of the increase in  $\epsilon^{\text{sph}}$ , the discussed specific features that are associated with the temperature dependence of the spectral absorption coefficient are tracked with increase in the radiating volume. Beginning with 1000 K and up to 2000–3000 K, the temperature increase leads to a decrease in  $\epsilon^{\text{sph}}$ , after which, up to the instant of complete gas ionization ( $T \sim 5000$  K), the fraction of opaque radiation increases maximally. A further increase in the temperature leads to the illumination of the plasma.

## NOTATION

$\vec{\Omega}$ , unit vector in the direction of quantum motion;  $I$ , radiation intensity;  $S$ , radiant energy flux;  $U$ , radiation density;  $K$ , absorption coefficient;  $K'$ , absorption coefficient with allowance for reradiation;  $l$ , radiation path length;  $k_{\text{pk}}$ , Planck mean value;  $l_{\text{Ros}}$ , Rosseland mean path length;  $\tau$ , optical thickness;  $\epsilon$ , emissivity;  $\epsilon^{\text{pl}}$  and  $\epsilon^{\text{sph}}$ , emissivities of the plane layer and of the hemispherical volume;  $\nu$ , frequency;  $\nu_{\text{thr}}$ , threshold frequency;  $\nu_0$ , line center;  $W$ , probability of level realization;  $\xi(\nu)$ , Biberman–Norman function;  $\Delta\nu_{\text{opt}}$ , optical shift of the photoionization threshold;  $\sigma_n$ , photoionization cross section;  $n_n$ , level population;  $\epsilon$ , energy of the level;  $S_{\text{line}}$ , line strength;  $f_{nj}$ , oscillator strength of the transition ( $n \rightarrow j$ );  $\Delta\nu$ , spectral interval;  $\Delta\nu_{\text{Dop}}$ , Doppler halfwidth;  $\Delta\nu_{\text{St}}$ , Stark halfwidth;  $\Delta\nu_{\text{nat}}$ , natural halfwidth;  $\Delta\nu_{\text{res}}$ , resonance halfwidth;  $\Delta\nu_{\text{imp}}$ , impact halfwidth;  $d_{\text{St}}$ , Stark shift;  $g_0$ , statistical weight of the ground state;  $g_{\text{tr}}$ , statistical weight of the transition level;  $n_0$ , concentration of atoms in the ground state;  $n_e$ , concentration of electrons;  $n_i$ , concentration of ions;  $n$ , concentration of initial atoms;  $\Sigma_0$ , statistical sum of the atom;  $\Sigma_1$ , statistical sum of the ion;  $\alpha$ , degree of ionization;  $I = 5.138$  eV, ionization potential of the Na atom;  $\mu = 22.991$ , atomic weight of Na;  $\Delta I$ , decrease in the ionization potential;  $E$ , electric field intensity;  $E_0 = (4\pi/3)^{1/2} \cdot en_i^{2/3}$ , mean intensity of the electric field;  $D = \sqrt{kT/4\pi e^2 n_i}$ ,

Debye radius;  $r_0 = (1/n_i)^{1/3}$ , mean distance between the ions;  $Z$ , charge number;  $Z^*$ , effective charge number of the atomic residue;  $T$ , temperature;  $p$ , pressure;  $e$ , electron charge;  $k$ , Boltzmann constant;  $h$ , Planck constant;  $m_e$ , mass of the electron;  $m$ , mass of the atom;  $c$ , speed of light;  $E_3(z) = \int_1^{\infty} \exp(-zx)dx/x^3$ , integral exponent.

Subscripts: v, spectral; veq, spectral equilibrium; vcon, spectral continuous; vline, spectral line;  $n$ ,  $n$ -th state ( $n$ -th transition); over, overall; opt, optical. Superscripts: pl, plane; sph, spherical.

## REFERENCES

1. Ya. B. Zel'dovich and Yu. P. Raizer, *Physics of Shock Waves and of High-Temperature Gasdynamic Phenomena* [in Russian], Moscow (1966).
2. A. N. Lagar'kov and I. T. Yakubov, *Opt. Spektrosk.*, **14**, No. 2, 199-207 (1963).
3. L. M. Biberman and G. E. Norman, *Usp. Fiz. Nauk*, **91**, No. 2, 193-246 (1967).
4. L. M. Biberman and G. E. Norman, *JQRST*, **3**, No. 1, 221-245 (1963).
5. V. G. Sevast'yanenko, *Radiative Heat Transfer in a Real Spectrum*, Doctoral Dissertation in Physical-Mathematical Sciences, Novosibirsk (1980).
6. G. A. Koval'skaya and V. G. Sevast'yanenko, in: *Properties of a Low-Temperature Plasma and Methods of Its Diagnostics*, Novosibirsk (1977), pp. 11-37.
7. V. G. Sevast'yanenko, *Effect of the Interaction of Particles in a Low-Temperature Plasma on Its Composition and Optical Properties*, Preprint Nos. 30 and 32 of the Institute of Theoretical and Applied Mechanics, Siberian Branch of the Academy of Sciences of the USSR, Novosibirsk (1980).
8. C. F. Hooper, *Phys. Rev.*, **165**, No. 1, 215-222 (1968).
9. L. P. Kudrin, *Statistical Physics of Plasma* [in Russian], Moscow (1974).
10. S. S. Katsnel'son and G. A. Koval'skaya, *Thermophysical and Optical Properties of an Argon Plasma* [in Russian], Novosibirsk (1985).
11. S. S. Penner, *Quantitative Molecular Spectroscopy and Radiating Power of Gases* [in Russian], Moscow (1963).
12. V. S. Matveev, *Zh. Prikl. Spektrosk.*, **14**, Issue 2, 228-233 (1972).
13. I. V. Avilova, L. M. Biberman, V. S. Vorob'ev, et al., *Optical Properties of a Hot Air* [in Russian], Moscow (1970).
14. Yu. V. Moskvina, *Opt. Spektrosk.*, **15**, No. 5, 582-586 (1963).
15. G. Grimm, *Plasma Spectroscopy* [Russian translation], Moscow (1969).
16. G. Grimm, *Broadening of Spectral Lines in Plasma* [Russian translation], Moscow (1978).
17. W. L. Wiese, M. W. Smith, and B. M. Glennon, *Atomic Transition Probabilities*, Vol. 2, Washington (1966).
18. E. M. Andersen and V. A. Zilitis, *Opt. Spektrosk.*, **16**, No. 2, 177-181 (1964).
19. L. I. Grekov, Yu. V. Moskvina, V. S. Romanychev, and O. N. Favorskii, *Basic Properties of Certain Gases at High Temperatures* [in Russian], Moscow (1964).